Biomaterials 35 (2014) 7101–7109

Contents lists available at ScienceDirect

Biomaterials

journal homepage: www.elsevier.com/locate/biomaterials

Targeting the thyroid gland with thyroid-stimulating hormone (TSH)-nanoliposomes

Donatella Paolino [a,i,1], Donato Cosco [a,i,1], Marco Gaspari [b], Marilena Celano [a], Joy Wolfram [c,d], Pasquale Voce [e], Efisio Puxeddu [e], Sebastiano Filetti [f], Christian Celia [c,g,i], Mauro Ferrari [c,h,***], Diego Russo [a,**], Massimo Fresta [a,i,*]

[a] Department of Health Sciences, University of Catanzaro "Magna Græcia", Campus Universitario "S. Venuta", Viale S. Venuta, Germaneto, I-88100 Catanzaro, Italy
[b] Department of Experimental and Clinical Medicine, University of Catanzaro"Magna Græcia", Campus Universitario "S. Venuta", Viale S. Venuta, Germaneto, I-88100 Catanzaro, Italy
[c] Department of Nanomedicine, Houston Methodist Research Institute, Houston, TX 77030, USA
[d] CAS Key Laboratory for Biomedical Effects of Nanomaterials & Nanosafety, National Center for Nanoscience & Technology of China, Beijing 100190, China
[e] Department of Internal Medicine, University of Perugia, 06123 Perugia, Italy
[f] Department of Internal Medicine and Medical Specialties, University of Rome "Sapienza", V.le del Policlinico, 155, 00161 Rome, Italy
[g] Department of Pharmacy, University of Chieti – Pescara "G. d Annunzio", Via dei Vestini 31, Chieti 66013, Italy
[h] Department of Medicine, Weill Cornell Medical College, New York, NY 10065, USA
[i] IRC FSH-Interregional Research Center for Food Safety & Health, University of Catanzaro "Magna Græcia", Campus Universitario "S. Venuta", Viale S. Venuta, Germaneto, I-88100 Catanzaro, Italy

ARTICLE INFO

Article history:
Received 6 March 2014
Accepted 18 April 2014
Available online 14 May 2014

Keywords:
Nanoliposomes
Nanoparticles
Targeting
Thyroid cancer
Thyroid gland

ABSTRACT

Various tissue-specific antibodies have been attached to nanoparticles to obtain targeted delivery. In particular, nanodelivery systems with selectivity for breast, prostate and cancer tissue have been developed. Here, we have developed a nanodelivery system that targets the thyroid gland. Nanoliposomes have been conjugated to the thyroid-stimulating hormone (TSH), which binds to the TSH receptor (TSHr) on the surface of thyrocytes. The results indicate that the intracellular uptake of TSH-nanoliposomes is increased in cells expressing the TSHr. The accumulation of targeted nanoliposomes in the thyroid gland following intravenous injection was 3.5-fold higher in comparison to untargeted nanoliposomes. Furthermore, TSH-nanoliposomes encapsulated with gemcitabine showed improved anticancer efficacy *in vitro* and in a tumor model of follicular thyroid carcinoma. This drug delivery system could be used for the treatment of a broad spectrum of thyroid diseases to reduce side effects and improve therapeutic efficacy.

1. Introduction

The field of targeted therapy was born from the introduction of the "magic bullet" concept, which entails the selective delivery of a drug to a tissue of interest [1]. The concept involves reducing side effect, broadening the therapeutic window and increasing drug efficacy, through the selective delivery of an agent to a specific site in the body. Such selectivity is especially desired for diseases characterized by a low therapeutic index, such as cancer. Among various approaches adopted for drug delivery [2–5], liposomes provide a strategy for improving the biopharmaceutical properties of drugs [6–8]. In particular, pegylated liposomes can avoid immunological recognition and rapid clearance by macrophages [9–11]. Accordingly, several liposomal formulations have gained clinical approval and many more are currently undergoing clinical trials [12]. In an attempt to achieve selectivity, antibodies that are specific for surface molecules on target cells have been conjugated to liposomes. For instance, an antibody fragment against the

* Corresponding author. Department of Health Sciences, University of Catanzaro "Magna Græcia", Campus Universitario "S. Venuta", Viale S. Venuta, Germaneto, I-88100 Catanzaro, Italy. Tel.: +39 0961 369 4118; fax: +39 0961 369 4237.
** Corresponding author. Tel.: +39 0961 3694121; fax: +39 0961 3694237.
*** Corresponding author. Department of Nanomedicine, Houston Methodist Research Institute, Houston, TX 77030, USA. Tel./fax: +1 (713) 441 8439.
E-mail addresses: mferrari@HoustonMethodist.org (M. Ferrari), d.russo@unicz.it (D. Russo), fresta@unicz.it (M. Fresta).
[1] These authors contributed equally to this paper.

http://dx.doi.org/10.1016/j.biomaterials.2014.04.088

human epidermal growth factor receptor 2 (HER2), frequently expressed in breast cancer, has been attached to liposomes [13]. Similarly, liposomes have been coated with the monoclonal antibody (mAb) 2C5, which binds to nucleosomes on the surface of cancer cells [14]. In addition, folate-moieties have been incorporated in supramolecular vesicular aggregates to obtain preferential uptake by cancer cells that express the folate receptor [15,16].

Although several tissue-specific antibodies have been conjugated to nanoparticles, there are several organs, such as the thyroid gland, that have not been the focus of targeted drug delivery. We propose a strategy for obtaining preferential accumulation of nanoparticles in the thyroid. Thyroid-stimulating hormone (TSH) has been attached to the surface of pegylated nanoliposomes with the aim of targeting the TSH receptor (TSHr). The TSHr is a glycoprotein G-protein-coupled receptor expressed in the plasma membrane of thyrocytes. This receptor binds to TSH with high affinity and specificity and mediates the ligands biological effects on the thyroid gland [17]. TSHr expression is maintained in most thyroid pathologies, including benign and malignant tumors [18–23]. More importantly, the receptor is also present in the majority of less differentiated and more aggressive tumors [18–23], making it an optimal target for the delivery of chemotherapeutics.

2. Materials and methods

2.1. Materials

1,2-dipalmitoyl-sn-glycero-3-phospocholine monohydrate (DPPC) and N-(carbonyl-methoxypolyethylene glycol-2000)-1,2-distearoyl-sn-glycero-3-phosphoethanolamine (DSPE-mPEG$_{2000}$) were purchased from Genzyme (Suffolh, UK). 1,2-distearoyl-sn-glycero-3-phosphoethanolamine-N-[PDP(methoxypolyethylene glycol-2000)] (DSPE-mPEG2000-PDP) was obtained from Avanti Polar (Alabaster, Alabama, USA). TSH (from human pituitary), N-(fluorescein-5-tiocarbamoyl)-1,2-dihexadecanoyl-sn-glycero-3-phosphoethanolamine triethylammonium salt (fluorescein-DHPE), 3-[4,5-dimethylthiazol-2-yl]-3,5-diphenyltetrazolium bromide salt (tetrazolium salt) and dithiothreitol (DTT) were purchased from Sigma Chemicals Co. (St. Louis, USA). F12-medium, minimum essential medium (MEM) with glutamine, trypsin/ethylenediaminetetraacetic acid (EDTA) solution (1×), fetal bovine serum (FBS) and penicillin–streptomycin solution were obtained from Gibco (Invitrogen Corporation, UK). [^{3}H]-cholesteryl hexadecyl ether ([^{3}H]CHE, 40 Ci/mmol) was obtained from Perkin Elmer-Italia (Monza, Italy). Chemicals, buffers, liquid chromatography-mass spectrometry (LC-MS)-grade water, formic acid, cholesterol and acetonitrile and proteomics grade trypsin were obtained from Sigma–Aldrich (St. Louis, MO). Integra Frits™ 75 μm bore internal diameter (ID), Pico Frits™ 50 μm ID and 10 μm tip ID were from New Objective (Cambridge, MA). Microflow tees, PEEK™ unions and tees were from Upchurch Scientific (Oak Harbor, WA). The stationary phase used for packing the nanoscale LC column was 3 μm C_{18} provided by Dr. Maisch (Entringen, Germany). Zip Tips™ with strong cation exchange (SCX) properties were purchased from Millipore (Billerica, MA). Oasis HLB 1 cc (10 mg) solid phase extraction (SPE) cartridges were from Waters (Milford, MA). Gemcitabine (2,2I-difluorodeoxycytidine) hydrochloride (HPLC purity >99%) was a gift from Eli-Lilly Italia S.p.A. (Sesto Fiorentino, Firenze, Italy), and was used without further purification. FTC-133 human follicular thyroid carcinoma cells were purchased from Sigma–Aldrich (S.r.l. Milan, Italy) and Chinese hamster ovary (CHO) cells were provided by ATCC (Teddington, Middlesex, UK).

2.2. Preparation of TSH-nanoliposomes

Nanoliposomes were made from DPPC/cholesterol/DSPEmPEG2000/DSPE-mPEG2000-PDP (6:3:0.6:0.4 M ratio). The lipid mixture (20 mg) was dissolved in a round-bottom flask, using a chloroform/methanol mixture (3:1 v/v). Fluorescein-labeled and radiolabelled nanoliposomes where obtained by adding fluorescein-DHPE (0.1% molar) or [^{3}H]CHE to the lipid mixture. The organic solvents were removed with a rotary evaporator (Büchi R-210 Switzerland), followed by overnight incubation in a Büchi T51 glass-drying oven connected to a vacuum pump. Multilamellar nanoliposomes were prepared by hydrating the lipid film with 1 mL of saline solution (NaCl 0.9% w/v) and performing three alternate cycles (3 min each) of heating at 58 °C (water bath) and vortex mixing at 700 rpm. To reduce the disulfide bond the nanoliposomes were incubated with a 50 mM DTT solution (1:2 v/v respectively) for 30 min. Excess DTT was then removed after centrifugation at 20,000 × g for 60 min at 4 °C with a Beckman Coulter Allegra 64R centrifuge. Successively, the pellet was resuspended in 250 mM ammonium sulfate solution (1 mL) and subjected to ten cycles of freezing (liquid nitrogen) and thawing (water bath at 40 °C), thus achieving a pH gradient with an acid environment in the aqueous compartment.

The nanoliposomes were further extruded through polycarbonate filters with pore sizes of 400 nm, 200 nm and 100 nm (Costar, Corning Incorporated, NY, USA) using a stainless steel extrusion device (Lipex Biomembranes, Vancouver, BC, USA). Unentrapped ammonium sulfate solution was removed by centrifugation. Gemcitabine loading was achieved by incubating nanoliposomes for 3 h at room temperature in an isotonic solution (1 mL) of gemcitabine-hydrochloride (1 mM). Unentrapped drug was removed by gel permeation chromatography. The 3-(2-pyridyldithio)propionate (PDP) moieties on the liposomal surface were reduced and conjugated to TSH (2.5 μg/mL nanoliposomes) through overnight incubation.

2.3. TSH-nanoliposome purification

Unentrapped gemcitabine and unconjugated TSH were removed by gel permeation chromatography using an ÄKTA prime PLUS (Amersham Biosciences, Uppsala, Sweden), equipped with an UV detector at fixed wavelengths (254 nm and 280 nm). The purification procedure was performed at room temperature using a XK16/20 column (Amersham Biosciences, Uppsala, Sweden) with Sephadex G-25 as the stationary phase and a saline solution as the eluent. The column had an equilibration volume of 80 mL and the flow rate was 0.5 mL/min. The amount of unentrapped gemcitabine was determined spectrophotometrically with λ_{max} (wavelength) at 268.8 nm using a Perkin Elmer Lambda 20 UV-Vis spectrophotometer (Uberlingen, Germany) equipped with Perkin Elmer UV WinLab™ ver. 2.8 acquisition software (Uberlingen, Germany).

2.4. Sample preparation for liquid chromatography-tandem mass analysis spectrometry

To obtain a reference value, human TSH (2.5 μg in 5 μL) was diluted with 20 μL of digestion buffer composed of 0.2% (v/v) SDS and 200 mM tris(hydroxymethyl)aminomethane (Tris, pH 8.5). The protein was reduced by adding 100 mM DTT (2.5 μL) and incubating the mixture for 1 h at 37 °C. Cysteines were then alkylated by adding 3 μL of 200 mM freshly prepared iodoacetamide solution in water and incubating the mixture for 1 h at 37 °C. Finally, excess iodoacetamide was neutralized by adding 0.5 μL of 100 mM DTT. The solution was brought to a volume of 100 μL by adding LC water, and trypsin was added (500 ng) to allow enzymatic digestion. Before performing LC coupled to tandem MS (LC-MS/MS) analysis, 3 μL of digested TSH was diluted with 27 μL of solution SCX1, composed of acetonitrile/water/formic acid (80:19.9:0.1 v/v/v), and purified by ZipTips SCX following a slightly modified procedure, with respect to the manufacturer's instructions. Briefly, ZipTips were equilibrated with solution SCX1 and then used to concentrate the peptide mixture through at least five cycles of aspiration/discarding (aspiration volume 10 μL). After 5 × 10 μL washes with solution SCX1, the detergent-free peptide mixture was eluted in 2 μL of water/methanol/ammonium hydroxide solution (80:15:5, v/v/v). The sample was then diluted in 28 μL of loading pump solvent.

In order to evaluate whether the conjugation of TSH hormone with nanoliposomes was successful, the formulation was washed three times and then incubated with DTT (10 mM) and Tris (100 mM). The supernatants from the last wash (control) and nanoliposomes incubated with DTT were analyzed. Proteins were reduced, alkylated, and digested, as described in the section above. The samples were concentrated by SPE. Briefly, the SPE column (beads, 10 mg) was conditioned with 500 μL of water/methanol 1/1 (v/v); the column was then equilibrated with 500 μl of water/methanol/trifluoroacetic acid (TFA) (97.9:2:0.1 v/v/v) (Wash RP1); the peptide solution was then acidified to 0.5% (v/v) TFA and loaded onto the SPE cartridge. After two consecutive 400 μL washes of Wash RP1 and a water/methanol/formic acid mixture (97.9:2:0.1 v/v/v), peptides were eluted off the SPE cartridge with 250 μL of water/methanol/formic acid (19.9:80:0.1 v/v/v). Samples were then evaporated in a vacuum centrifuge, and reconstituted in 30 μL of loading pump solvent.

2.5. LC-MS/MS analysis and database search

Chromatography was performed on an Ultimate Nano LC System from Dionex (Sunnyvale, CA) using a valveless setup [24]. 10 μL of sample was loaded in an in-house packed 75 μm ID, 4 cm long Integra Frit™ trapping column (1 cm packing bed length) at 12 μL/min of loading pump solvent consisting of water/acetonitrile/trifluoroacetic acid (TFA) (97.95:2:0.05 v/v/v). After 4 min of washing, the trapping column was switched online to the analytical in-house packed 50 μm ID, 12 cm long Pico Frit™ column filled with 3 μm C_{18} silica particles, and gradient separation was started at 100 nL/min. A binary gradient was used for peptide elution. The mobile phase A consisted of water/acetonitrile/formic acid/TFA (97.9:2:0.09:0.01 v/v/v/v), while the mobile phase B consisted of water/acetonitrile/formic acid/TFA (29.9:70:0.09:0.01 v/v/v/v). Gradient conditions were 5% (v/v) B to 45% (v/v) B in 25 min. After 5 min at 95% (v/v) B, the column was re-equilibrated at 5% (v/v) B for 20 min before the next injection.

MS detection was performed on a QSTAR XL hybrid LC-MS/MS from Applied Biosystems (Foster City, CA), operating in positive ion mode with electro-spray potential at 1800 V, curtain gas at 15 units and collisionally activated dissociation (CAD) gas at 3 units. Information dependent acquisition (IDA) was done by selecting the four most abundant peaks for analysis after a full time of flight (TOF)-MS scan

from 350 to 1400 m/z lasting 3 s. The threshold value for the peak selection for MS/MS was 25 counts. MS/MS analysis was performed in enhanced mode (3 s/scan).

Data were searched on the Mascot search engine (www.matrixscience.com) against the SwissProt database using the following parameters: MS tolerance 100 ppm; MS/MS tolerance 0.3 Da; fixed modifications carbamidomethyl cysteine; variable modifications methionine oxidized; enzyme trypsin; maximum missed cleavages 2; taxonomy human.

2.6. Physicochemical characterization of TSH-nanliposomes

The physicochemical properties of TSH-nanoliposomes were characterized using a Zetasizer Nano ZS (Malvern Instruments Ltd., Worchestershire, United Kingdom) as previously reported [7]. Briefly, samples were diluted 1:50 in isotonic saline solution (NaCl 0.9% w/v) to avoid multiscattering. The average size and narrow size distribution was measured using photon correlation spectroscopy. The instrument was equipped with a 4.5 mW laser diode operating at 670 nm. Scattered photons were detected at 173°. The third-order cumulant fitting autocorrelation function was applied to achieve mean sizes and size distribution profiles from scattered photon patterns. The following parameters were used: real refractive index 1.59, imaginary refractive index 0.0, medium refractive index 1.330, medium viscosity 1.0 mPa × s and medium dielectric constant 80.4. The zeta potential was measured using the Doppler laser anemometry. The apparatus was equipped with a He/Ne laser doppler anemometry (633 nm) with nominal power of 5.0 mW. A Smoluchowsky constant F (Ka) of 1.5 was applied during analysis. For each sample five measurements were taken with 15 runs per measurement. Results are the average ± standard deviation.

For freeze fracture electron microscopy analysis, samples were centrifuged at 30,000 × *g* for 30 min at room temperature (Microcentrifuge Ole Dich. Denmark), impregnated with 30% (v/v) glycerol, and then frozen in partially solidified Freon 22. The samples were freeze fractured in a freeze fracture device (105 °C, 10-6 mm Hg) and replicated by evaporation from a platinum/carbon gun. The replicas were extensively washed with distilled water, picked up onto Formvar coated grids and examined with a Philips CM 10 transmission electron microscope, as previously reported [25].

2.7. Cell culture

To evaluate the selectivity of the TSH-nanoliposomes against cells expressing the TSHr, CHO wild type cells without TSHr (CHO-w) and CHO cells transfected with TSHr (CHO-t) were used. TSHr transfection was performed as previously reported [26]. CHO cells were incubated (Guaire® TS Autoflow Codue Water-Jacketed-Incubator) with F12 medium containing penicillin (100 UI/mL), streptomycin (100 μg/mL) and FBS (10%, v/v). FTC-133 human thyroid carcinoma cells were incubated with DMEM/F12 (1:1 v/v) supplemented with glutamate, D-glucose, pyruvate, 10% FBS (v/v), penicillin (100 UI/mL), and streptomycin (100 μg/mL). The medium was replaced every 48 h.

2.8. Intracellular accumulation of TSH-nanoliposomes

The intracellular accumulation of radiolabeled [^{3}H]CHE TSH-nanoliposomes and control nanoliposomes in CHO-w cells (do not express TSHr) and CHO-t cells (express TSHr) was measured as a function of time. [^{3}H]CHE was used at a concentration of 0.003% v/v, which corresponds to 3 nmol of [^{3}H]CHE. Cells were plated in 6-well culture dishes (5×10^5 cells/ml) and successively treated with 100 μl of tritiated nanoliposomes. Free TSH (0.1-1000 μU/mL) was used in order to investigate competitive binding to the hormone receptor. After a 3 h incubation period, cells were centrifuged (1200 rpm at room temperature for 10 min) and the culture medium was removed. Cells were washed twice with phosphate buffered saline (PBS) and transferred into polypropylene liquid scintillation vials (Sigma–Aldrich Chemie, GmbH, Steinheim, Germany). Cells were then dissolved in a quaternary ammonium hydroxide solution (2 mL, BTS-450, Beckman Instruments, Inc., Fullerton, Netherlands) under continuous shaking for 1 h at 60 °C, using an incubator shaker (Innova™ 4300, New Brunswick Scientific, Edison, NJ, USA). At the end of the incubation time, the liquid scintillation cocktail (7 mL, Ready Organic™, Beckman Coulter Inc., Fullerton, USA) was added to the solution and the samples were vigorously mixed and analyzed using a Wallac Win Spectral™ 1414 liquid scintillation counter (PerkinElmer Life and Analytical Sciences, Inc. Waltham, MA, USA). 1414 Win Spectral Wallac LCS Software was used for data analysis.

2.9. Confocal laser scanning microscopy

The intracellular uptake of fluorescein-labeled TSH-nanoliposomes was measured in CHO and FTC-133 cells using confocal laser scanning microscopy (CLSM). Cells (4×10^5 cells/ml) were placed in 6-well culture plates with culture medium and a sterile glass slide was positioned in each well. Plates were incubated for 24 h followed by treatment with fluorescein-labeled nanoliposomes for 2 h. Each well was then washed with PBS (3 times) to remove excess nanoliposomes and cells were fixed on a sterile glass slide, using 1 mL of an ethanol solution (70%, v/v). Each slide was washed again with PBS (3 times) and treated with 1 mL of Hoechst solution (1/1000), incubated for 5 min and then washed with PBS (3 times, 2 mL). Plates were stored at 4 °C prior to CLSM analysis. CLSM was carried out using a Leika TCS SP2 MP CLSM operating at $\lambda_{exc} = 496$ nm and $\lambda_{em} = 519$ nm for the FITC probe and at $\lambda_{exc} = 405$ nm and $\lambda_{em} = 460$ nm for the Hoechst probe. A scan resolution of 4096 × 4096 pixels with an Ar/Kr laser beam of 75 mW, equipped with a fluorescein analyzer filter, was used for imaging. Samples were recorded with a macro developer software package with multi-dimensional series acquisition and direct access digital control knobs. An immersion oil lens of 63× was used.

2.10. In vitro anticancer activity

The *in vitro* anticancer activity of free gemcitabine and gemcitabine-loaded nanoliposomes or TSH-nanoliposomes was evaluated using a MTT assay. Cells were plated into 96-well culture dishes (5×10^3 cells/0.2 mL) and incubated for 24 h. Cells were then treated with free drug or nanoliposomes (8 wells/group) and incubated for 24 h, 48 h or 72 h. Untreated cells were used as a control. Cells were then incubated for 3 h in tetrazolium salt dissolved in PBS solution (10 μL, 5 mg/mL). The medium was removed and formazan crystals, which precipitated at the bottom of the well after mitochondrial oxidation, were dissolved with 200 μL of a DMSO/ethanol mixture (1:1, v/v) and mixed for 20 min at 230 rpm (IKA® KS 130 Control, IKA® WERKE GMBH & Co., Staufen, Germany). The solubilized formazan crystals were quantified with a microplate spectrophotometer (Multiskan MS 6.0, Labsystems) at a wavelength of 540 nm with a reference wavelength of 690 nm. The percentage of viable cells was calculated according to the following equation:

$$\text{Cell viability}(\%) = Abs_T/Abs_C \times 100$$

where Abs_T is the absorbance of the treated cells and Abs_C is the absorbance of control (untreated) cells. The mean cell viability ± standard deviation was derived from six independent experiments.

2.11. Intracellular uptake of gemcitabine

CHO-w and CHO-t cells were seeded in 12-well plates (3×10^4 cells/mL) and incubated with free gemcitabine, gemcitabine-loaded TSH-nanoliposomes or gemcitabine-loaded untargeted nanoliposomes at a final concentration of 1 μM. At various time points, the cells were scraped from the wells, collected and centrifuged (1200 rpm, 10 min, 22 °C). The pellets were then resuspended in PBS (1 mL) and disrupted by sonication (SONOPOLUS GM 70, Bandelin Electronic, Berlin, Germany) at 50 cycles per second for 3 min. The intracellular amount of gemcitabine was determined by LC. The mean was calculated from five independent experiments. Each sample was prepared for LC analysis by adding a 2% (w/v) zinc sulfate solution (1.4 mL) in a methanol/water mixture (30:70 v/v). The solution was vortex mixed for 5 min and then centrifuged at 6000 rpm with an Eppendorf Megafuge centrifuge (BJB Labcare Ltd., Buckinghamshire, United Kingdom). The supernatant was filtered through a nylon membrane with a pore size of 0.22 μm (Whatman Inc.), lyophilized, dissolved in 100 μL of the mobile phase and subjected to LC analysis.

2.12. LC quantification

LC analysis was performed using a system from Varian Inc. (Palo Alto, CA, USA), composed of a 200-2031 Metachem online degasser, a M210 binary pump, a ProStar 410 autosampler, a G1316A thermostat column compartment and a 25 μL CSL20 Cheminert Sample Loop injector. Data was acquired and processed with a Galaxie® chromatography manager software (Varian Inc.). Chromatographic separation was carried out at room temperature using a GraceSmart RP C18 column (4.6 × 250 mm, 5 μm particle size, Alltech Grom GmbH, Rottenburg-Hailfingen, Germany). The mobile phase was water/acetonitrile (95:5 v/v). The flow rate was 1 mL/min and detection was performed at wavelength of 269 nm.

Quantification of gemcitabine was done using a standard curve in the linear concentration range of 0.1 ng/mL to 10 μg/mL. The amount of gemcitabine was determined according to the following equation:

$$\text{AUC} = 0.60112x + 0.02840$$

where x is the drug concentration (μg/mL) and AUC the area under the curve (mAu × min).

2.13. Animals

In vivo experiments were performed according to the principles and procedures outlined by the local Ethical Committee and the European Communities Council Directive of 24 November 1986 (86/609/EEC). Animals were maintained at standard temperature (20 ± 2 °C) and humidity (65%) conditions with 12 h light/12 h dark cycles and food and water *ad libitum*. Wistar rats and nonobese diabetic/severe combined immunodeficiency (NOD/SCID) mice were purchased from Harlam (Italy s.r.l. San Pietro al Natisone (UD), Italy).

2.14. In vivo biodistribution

Biodistribution experiments were performed in female Wistar rats (4–5 months old, 200–250 g). [^{3}H]CHE-radiolabeled (0.003% v/v corresponding to 3 nmol of [^{3}H]CHE) nanoliposomes were injected through the tail vein (200 μL). After 3 h, the rats were sacrificed by cervical dislocation and organs were collected. Organs were

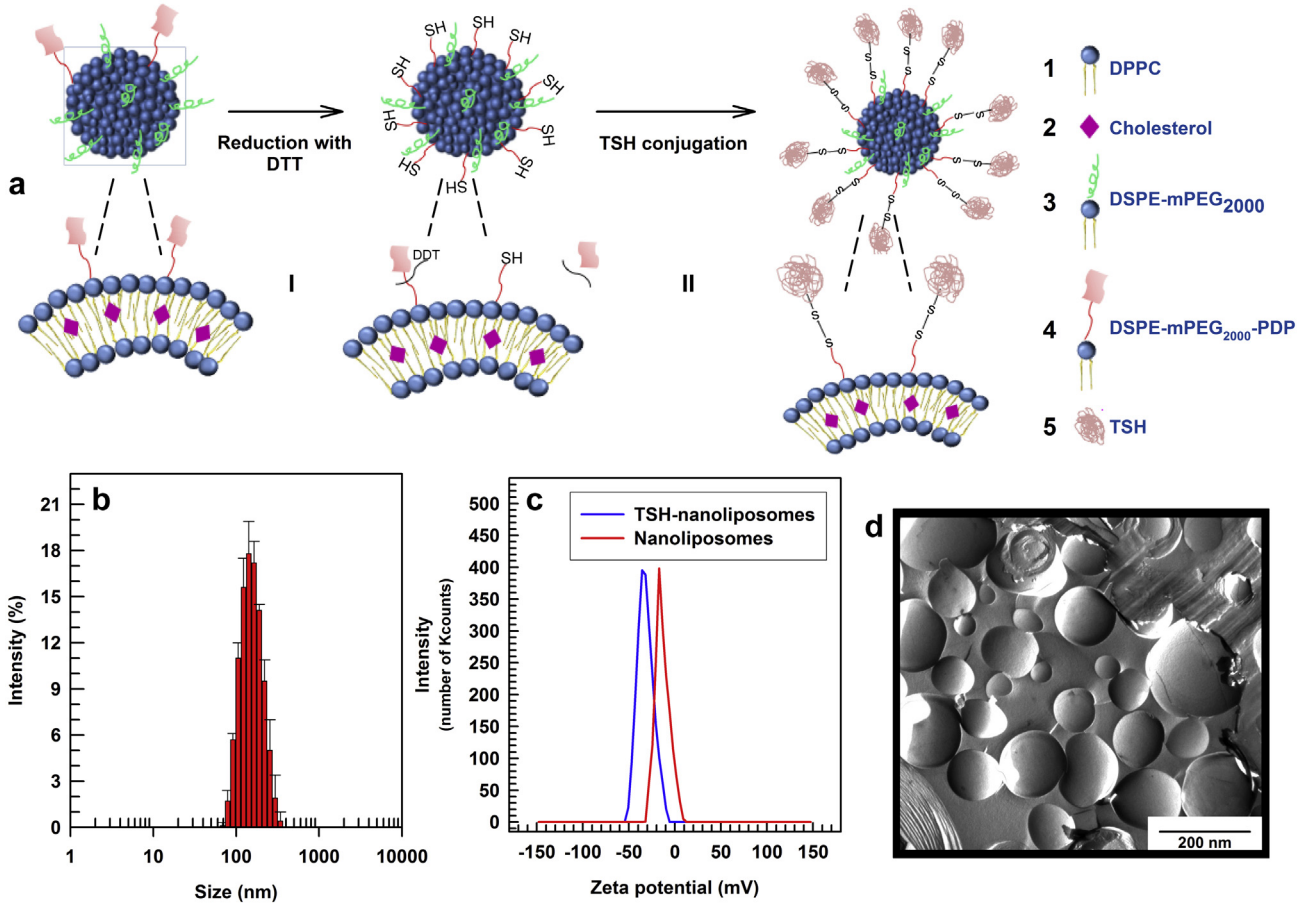

Fig. 1. Preparation and physicochemical characterization of thyroid-stimulating hormone (TSH)-nanoliposomes. (a) Schematic representation of TSH conjugation to the surface of nanoliposomes. (I) The 3-(2-pyridyldithio)propionate (PDP)-moieties present on the surface of the unilamellar vesicles were reduced using dithiothreitol (DTT), resulting in the formation of vesicles with −SH groups on their surface. (II) TSH-nanoliposomes were formed through the conjugation of TSH with −SH functional moieties on the lipid surface. (b) Mean size and size distribution of TSH-nanoliposomes measured with photon correlation spectroscopy. (c) Zeta potential analysis of nanoliposomes. (d) Freeze-fracture transmission electron microscopy of TSH-nanoliposomes. DPPC, 1,2-dipalmitoyl-sn-glycero-3-phospocholine monohydrate; DSPE-mPEG$_{2000}$, N-(carbonyl-methoxypolyethylene glycol-2000)-1,2-distearoyl-sn-glycero-3-phospho-ethanolamine; DSPE-mPEG$_{2000}$-PDP, 1,2-distearoyl-sn-glycero-3-phosphoethanolamine-N-[PDP(methoxypolyethylene glycol-2000)].

transferred into polypropylene liquid scintillation vials (Sigma–Aldrich Chemie, GmbH, Steinheim, Germany) and mixed with a quaternary ammonium hydroxide solution (2 mL) (BTS-450, Beckman Instruments, Inc., Fullerton, Netherlands) under continuous shaking for 4 h at 60 °C using an incubator shaker (Innova™ 4300, New Brunswick Scientific, Edison, NJ, USA) to allow complete dissolution. Samples were then decolorized with 2 mL of 24% (v/v) H_2O_2 at room temperature for 5 min. The liquid scintillation cocktail (7 mL) (Ready Organic™, Beckman Coulter Inc., Fullerton, USA) was then added to the vials and the solution was vigorously mixed. The samples were analyzed using a Wallac Win Spectral™ 1414 liquid scintillation counter (PerkinElmer Life and Analytical Sciences, Inc. Waltham, MA, USA). 1414 Win Spectral Wallac LCS Software was used for data analysis. To correct for radioactivity derived from the blood, macrophages and capillary endothelial cells in the organs, a correction was made according to the following equation:

$$X_{tissue} = X_{organ} - (V_0 \times C_t)$$

where X_{tissue} represents the corrected radioactivity; X_{organ} represents the level of radioactivity recovered from the organ samples; V_0 stands for the total volume of the vascular space and interstitial fluid, as determined by the radioactivity level in the whole organ sample divided by the blood concentration 10 min after *i.v.* injection of [^{3}H]CHE-labeled nanoliposomes; and C_t represents the blood concentration at the indicated time. A further quenching correction factor was obtained by measuring the radioactivity of tissue samples from untreated rats spiked with known amounts of [^{3}H]CHE (0.030 μCi/μmol lipids).

2.15. In vivo anticancer efficacy and tumor accumulation

FTC-133 cells (1×10^6 cells/mL) were cultured using a previously reported protocol [27] and diluted into 200 μL of sterile isotonic PBS (Harlan Italy S.r.l., San Pietro al Natisone (UD), Italy). The cells were injected subcutaneously into female NOD SCID mice (4–6 weeks old, 20–22 g) and treatment was initiated when the average tumor volume reached ~500 mm^3 (~8–10 mm in diameter). Mice were divided into the following five treatment groups (5 mice/group): PBS, gemcitabine, gemcitabine-loaded nanoliposomes, and gemcitabine-loaded TSH-nanoliposomes. Free gemcitabine and both formulations containing gemcitabine nanoliposomes were administered intravenously (200 μL) at a gemcitabine dose of 5 mg/kg/day for 14 days. The tumor volume was measured every two days according to the following equation:

$$Vt = 0.5 \times D \times d^2$$

where *Vt* is tumor volume, *D* and *d* are the long and short tumor diameter. Mice were sacrificed and tumors were collected 15 days after treatment initiation.

Tumor accumulation studies were performed using the same tumor model as in the anticancer efficacy studies. When the average tumor volume reached ~500 mm^3 (~8–10 mm in diameter), mice were injected through the tail vein (200 μL) with [^{3}H]CHE-radiolabeled (0.003% v/v corresponding to 3 nmol of [^{3}H]CHE) TSH-nanoliposomes and control nanoliposomes. Mice were sacrificed at 1 h, 2 h, 8 h or 24 h post-injection. At each time point, the tumors from three mice per group were processed and analyzed as described in the *in vivo* biodistribution section.

3. Results and discussion

3.1. Synthesis and assembly of TSH-nanoliposomes

TSH-nanoliposomes were prepared by conjugating the amino acid residue of cysteine in the TSH hormone with a thiol-activated moiety present on the surface of the nanoliposome,

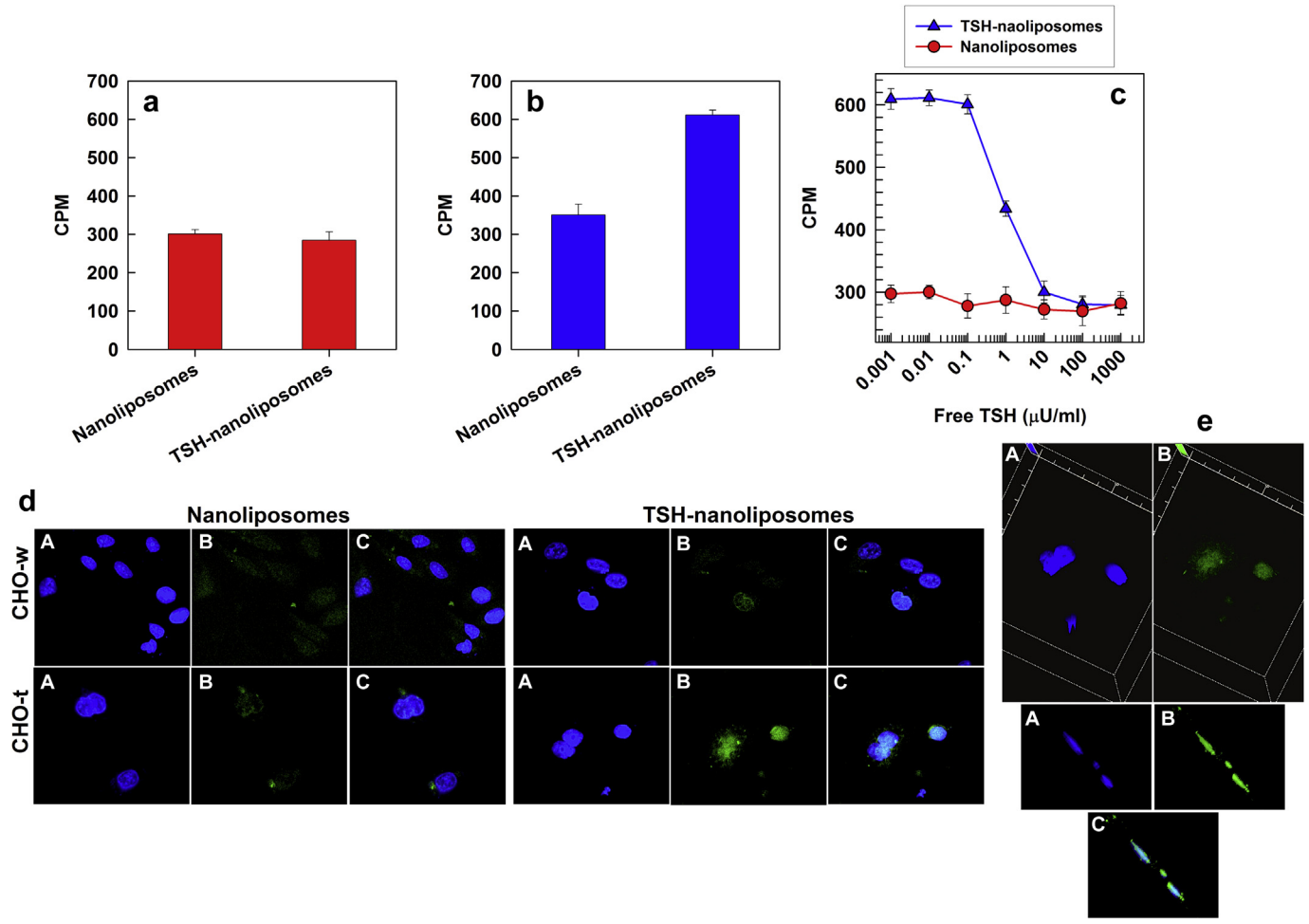

Fig. 2. Evaluation of the selectivity of TSH-nanoliposomes for TSH-receptor (TSHr)-expressing cells. Uptake of [^{3}H]CHE-radiolabeled TSH-nanoliposomes and un-conjugated nanoliposomes in chinese hamster ovary (CHO) cells without (CHO-w) (a) and with (CHO-t) the TSHr (b). (c) Competitive binding experiments in CHO-t cells using [^{3}H]CHE-radiolabeled TSH-nanoliposomes and control nanoliposomes in the presence of free TSH. (d) Confocal laser scanning microscopy of fluorescein-labeled TSH-nanoliposomes and control nanoliposomes after 2 h of incubation with CHO-w and CHO-t cells. Filter: Hoechst filter (DAPI) (A), FITC filter (B) and overlay (C). (e) 3D visualization of CHO-t cells after 2 h of incubation with TSH-nanoliposomes (upper two micrographs) and corresponding 3D visualization following a 180° rotation. Autofluorescence was not observed.

thereby forming a disulfide bond (Fig. 1). The formation of the conjugate was confirmed with LC-MS/MS (Supplementary Figs. S1 and S2). A small aliquot of pure TSH was digested and analyzed to generate a list of TSH specific peptides detectable by mass spectrometry. A database search of MS/MS data allowed for high-confidence identification of four specific peptides, three of which belonged to the alpha-subunit and one of which belonged to the beta-subunit (Supplementary Table S1). Selected ion chromatograms (SICs) for two out of the four peaks could be detected in the nanoliposome sample, whereas none of the peaks were present in the control sample. The amount of TSH peptide recovered from the nanoliposome surface was probably below the detection limit for the two peaks that did not show up during analysis. Supplementary Figs. S1 and S2 show SICs of those m/z giving a positive signal, which were ions at m/z 419.73 (peptide VTVMGGFK, belonging to alpha-chain of the TSH) and 688.32 (peptide ALSQDVCTYR, belonging to the beta-chain of the TSH). Moreover, the MS/MS spectrum acquired under the peak in data-dependent mode (Supplementary Figs. S1c and S2c) strongly resembles that of the MS/MS spectrum acquired from standard human TSH (Supplementary Figs. S1d and S2d). The data indicates that TSH was successfully conjugated to the surface of nanoliposomes.

3.2. Physicochemical characterization of TSH-nanoliposomes

A small size and a narrow size distribution is desired for colloidal drug delivery systems [28,29]. Here, photon correlation spectroscopy showed that the untargeted nanoliposomes and the TSH-nanoliposomes had a mean diameter of 141.8 nm (Supplementary Fig. S3) and 148.2 nm (Fig 1b), respectively. The small size increase following TSH conjugation suggests that thy hydrodynamic radius was increased due to the presence of an additional hydrophilic molecule on the liposomal surface. Furthermore, freeze-fracture transmission electron microscopy was performed to confirm the size-range of the particles (Fig. 1d). Gemcitabine-loaded nanoliposomes were not separately characterized, as it has previously been show that gemcitabine encapsulation does not affect the mean size and size distribution of vesicular carriers [30]. Both targeted and untargeted formulations exhibited a narrow size distribution (Fig 1b and Supplementary Fig. S3). The addition of TSH to the

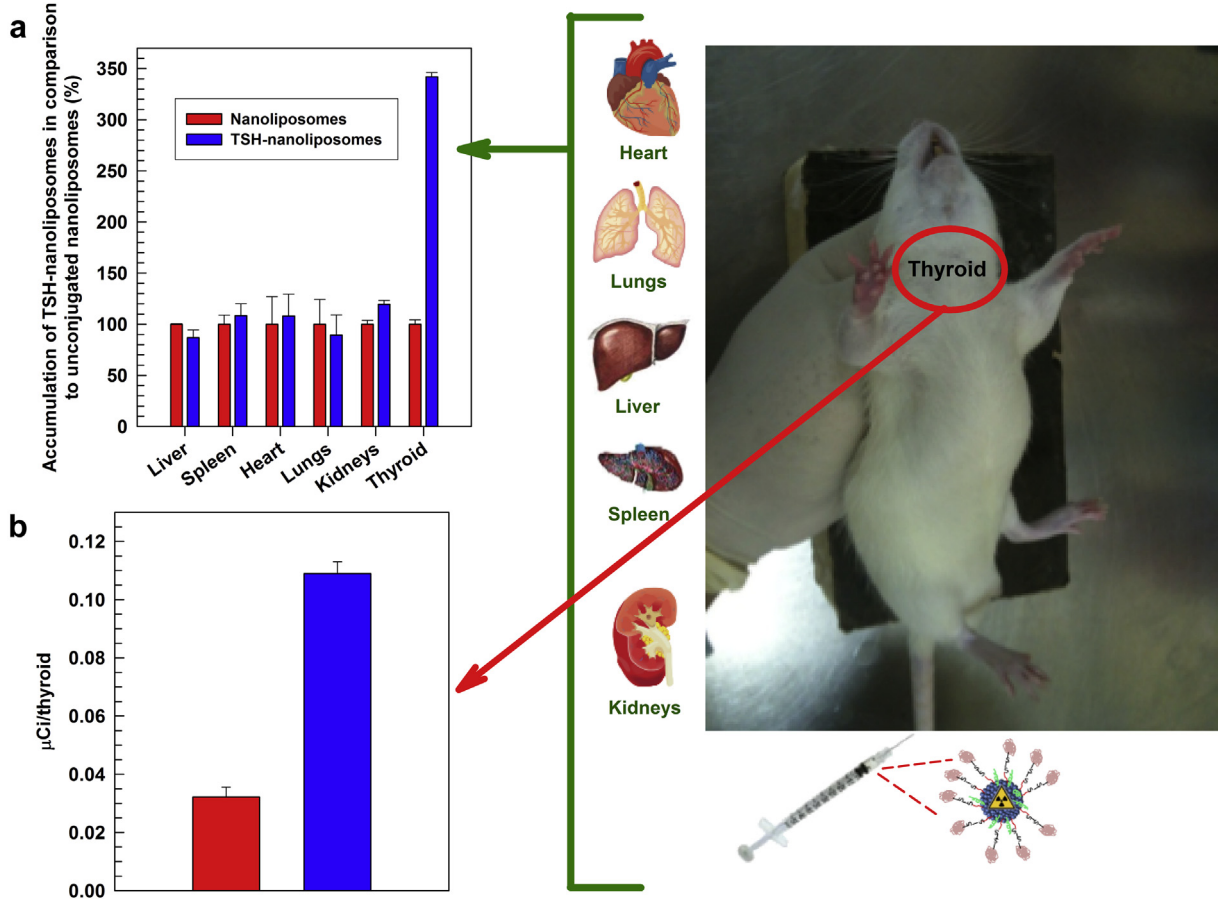

Fig. 3. *In vivo* biodistribution and thyroid uptake of TSH-nanoliposomes in Wistar rats. (a) Biodistribution of [^{3}H]CHE-radiolabeled TSH-nanoliposomes and control nanoliposomes. The nanoliposomes were injected through the tail vein of Wistar rats and various organs were collected 6 h after injection. (b) Quantification of nanoliposomes in the thyroid.

nanoliposomes influenced the surface characteristics of the vesicular carrier, resulting in a reduction of the zeta potential from −15 mV to −34 mV (Fig. 1c).

3.3. Intracellular uptake and in vitro cytotoxicity of TSH-nanoliposomes

The selectivity of TSH-nanoliposomes for cells expressing the TSHr was evaluated in wild-type CHO cells lacking the TSHr (CHO-w) and in CHO cells transfected with the TSHr (CHO-t). [^{3}H]CHE-radiolabeled TSH-nanoliposomes displayed enhanced cellular uptake in CHO-t cells in comparison to CHO-w cells, while the uptake of untargeted nanoliposomes was similar in both cell lines (Fig. 2a and b). Experiments evaluating the competitive binding of free TSH and nanoliposomes with TSHr on the cell surface were carried out using increasing doses of TSH (Fig. 2c). In the case of TSH-nanoliposomes, the cellular uptake in CHO-t cells decreased as the dose of free TSH increased, while the cellular internalization of unconjugated nanoliposomes was independent of free TSH. Accordingly, confocal laser scanning microscopy showed that fluoresceine-labeled TSH-nanoliposomes were internalized to a greater extent in CHO-t cells, as compared to untargeted nanoliposomes (Fig. 2d). These findings demonstrate the active targeting ability of the TSH-nanocarrier on the cellular level.

The cytotoxicity of empty TSH-nanoliposomes and control nanoliposomes was evaluated in CHO cells. The results indicate that the empty delivery system does not reduce cell viability (Supplementary Fig. S4). The cell viability remained over 95%, even when the empty nanoliposome was administered at high concentrations, demonstrating the *in vitro* biocompatibility of the delivery system.

3.4. Comparative biodistribution of TSH-nanoliposomes and control nanoliposomes

The comparative biodistribution of [^{3}H]CHE-radiolabeled TSH-nanoliposomes and control nanoliposomes in Wistar rats was evaluated. The results demonstrate a three-fold increase in the accumulation of the TSH-nanoliposomes in the thyroid, as compared to the untargeted nanoliposomes (Fig. 3). The conjugation of TSH to the liposomal surface did not increase the accumulation of nanoliposomes in other organs, including the liver, spleen, heart, lungs and kidney (Fig. 3), thus demonstrating *in vivo* selectivity for the TSHr in the thyroid gland.

3.5. In vitro anticancer efficacy of gemcitabine-loaded TSH-nanoliposomes

Next, TSH-nanoliposomes were evaluated as drug delivery systems for gemcitabine, an anticancer drug widely investigated as a candidate for liposomal delivery [15,16,27,30–32]. The cytotoxicity of this chemotherapeutic agent was examined *in vitro* in CHO cells, which were transfected with TSHr and in FTC-133 cells, which endogenously express TSHr. In general, gemcitabine-loaded nanoliposomes displayed greater anticancer efficacy to that of the free drug (Fig. 4 and Supplementary Fig. S4). In CHO-w cells there was

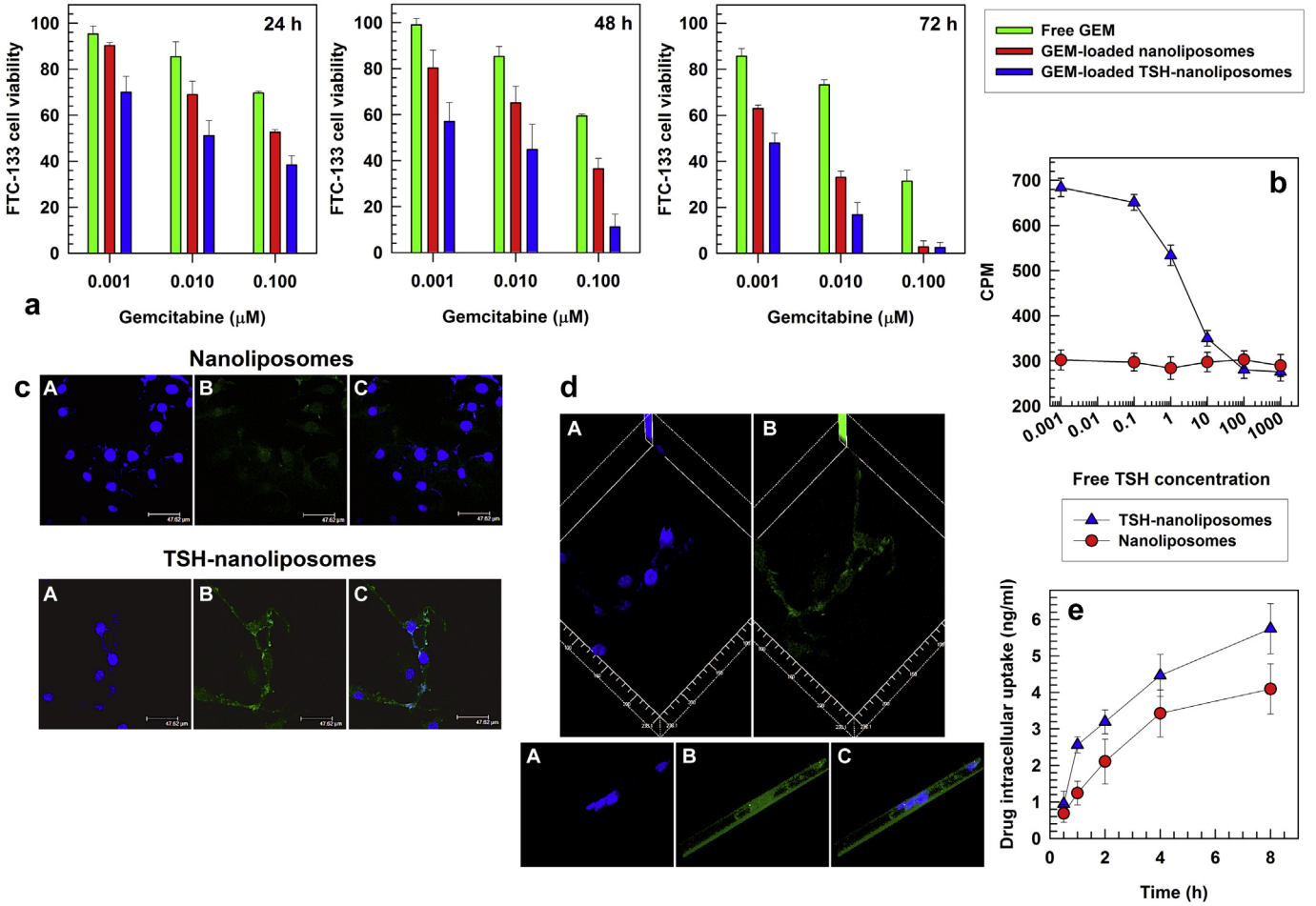

Fig. 4. Anticancer efficacy of gemcitabine (GEM)-loaded TSH-nanoliposomes in FTC-133 cells expressing the TSHr. (a) Time and dose-dependent effects of free GEM, GEM-loaded TSH-nanoliposomes and GEM-loaded control nanoliposomes in FTC-133 cells. (b) Competitive binding experiments in FTC-133 with [^{3}H]CHE-radiolabeled TSH-nanoliposomes and control nanoliposomes in the presence of free TSH. (c) Confocal laser scanning microscopy of FTC-133 cell incubated for 2 h with fluorescein-labeled nanoliposomes. Filters: Hoechst filter (DAPI) (A), FITC filter (B) and overlay (C). (d) 3D visualization of FTC-133 cells after 2 h of incubation with TSH-nanoliposomes (upper two micrographs) Corresponding 3D visualization following a 180° rotation (lower three micrographs). (e) Intracellular uptake of GEM encapsulated in TSH-nanoliposomes or control nanoliposomes. CPM, counts per minute.

no apparent difference between the cytotoxicity of gemcitabine-loaded targeted or untargeted nanoliposomes (Supplementary Fig. S4). However, in CHO-t cells the TSH-nanoliposomes outperformed the control nanoliposomes, in terms of reducing cell viability. For instance, after 72 h at a concentration of 1 μM gemcitabine, cells incubated with targeted nanoliposomes and untargeted nanoliposomes had a cell viability of ~28% and ~56%, respectively (Supplementary Fig. S4). Similarly, in FTC-133 cells, after 48 h at a concentration of 0.1 μM gemcitabine, cells incubated with TSH-nanoliposomes and control nanoliposomes had a cell viability of 11% and 36%, respectively (Fig. 4a). In this context, it was also demonstrated that the conjugation of TSH to nanoliposomes increased their intracellular uptake in FTC-133 cells (Fig. 4b–d). Accordingly, the intracellular concentration of gemcitabine also increased when targeted nanoliposomes were used as a delivery vehicle in comparison to untargeted nanoliposomes (Fig. 4e). Moreover, the intracellular accumulation of TSH-nanoliposomes decreased as the concentration of free TSH increased in the media (Fig. 4b). Competitive binding with the free ligand confirms that the major mechanism for cellular internalization is mediated by binding of the delivery system to TSHr. The results demonstrate that the conjugation of TSH can markedly improve the anticancer efficacy of gemcitabine-loaded nanoliposomes in cells expressing TSHr.

3.6. In vivo anticancer activity and tumor accumulation of gemcitabine-loaded TSH-nanoliposomes

A subcutaneous tumor model of follicular thyroid carcinoma (FTC-133 cells) was used to evaluate the *in vivo* anticancer efficacy of gemcitabine-loaded TSH-nanoliposomes. The nanoliposomes were radiolabeled ([^{3}H]CHE) to measure tumor accumulation upon intravenous injection. As is evident from Fig. 5a, the presence of the TSH on the liposomal surface allowed for increased accumulation of the delivery vehicle in the tumor. For instance, 1 h post administration, the TSH-nanoliposomes were present in the tumor at an almost two-fold higher level than the unconjugated nanoliposomes. Furthermore, the *in vivo* anticancer activity of gemcitabine-loaded nanoliposomes was evaluated. Gemcitabine-loaded TSH-nanoliposomes elicited the greatest reduction in tumor growth. Indeed, after 14 days of treatment, a significant difference in tumor volume and weight was evident between groups receiving gemcitabine-loaded TSH-nanoliposomes or gemcitabine-loaded control nanoliposomes (Fig. 5b and c). The anticancer efficacy is further illustrated in photographs of dissected tumor samples (Fig. 5d).

Taken together, the results demonstrate that TSH-nanoliposomes are an effective delivery platform for targeting thyroid tissue *in vivo*. We envision that TSH-nanoliposomes could

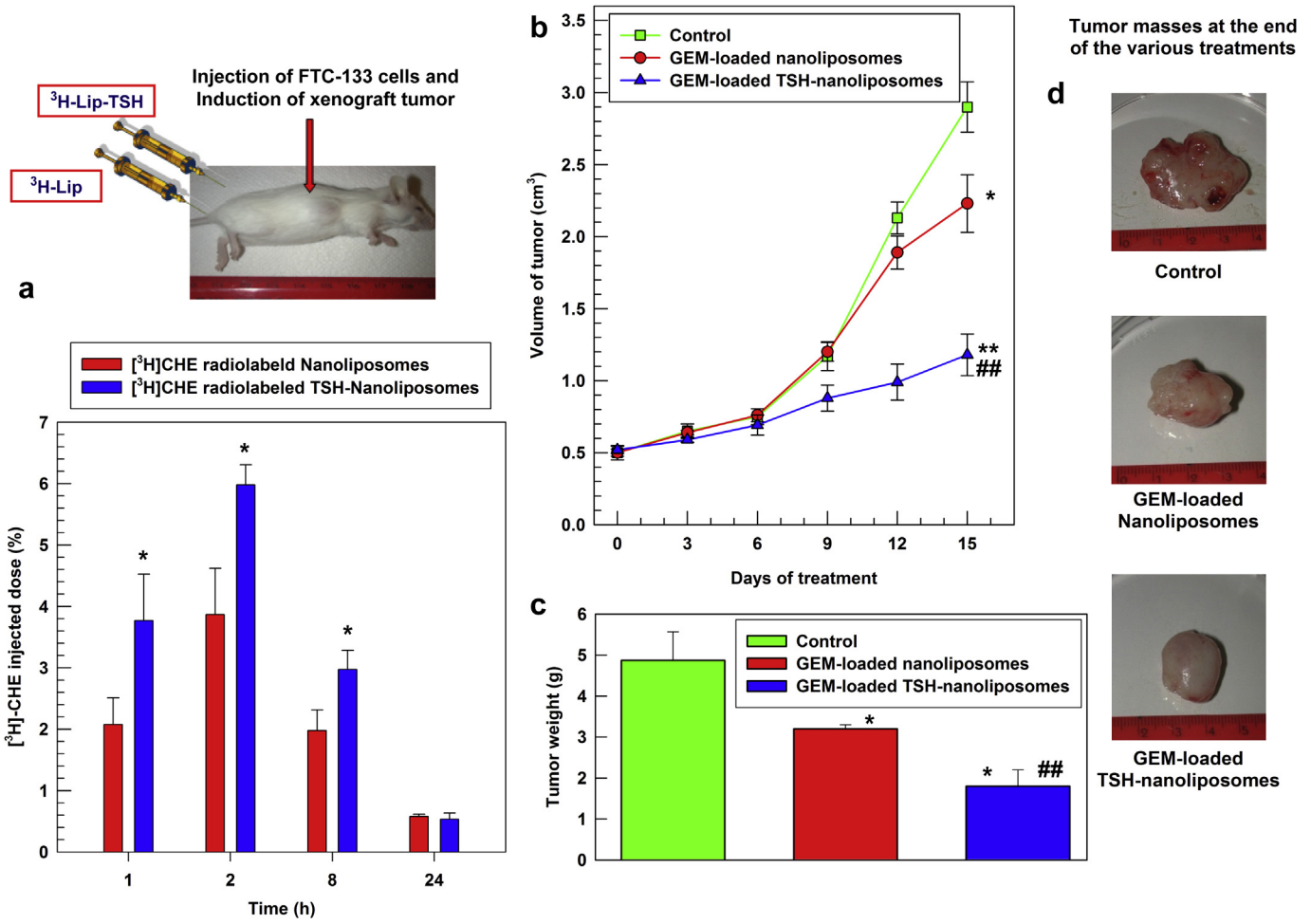

Fig. 5. *In vivo* anticancer efficacy and tumor accumulation of TSH-nanoliposomes in a tumor model of follicular thyroid carcinoma (FTC-133 cells). (a) *In vivo* tumor uptake of [^{3}H]-CHE radiolabeled TSH-nanoliposomes and control nanoliposomes ($n = 3$/group/time point). Statistical analysis was performed by one-way ANOVA and $p < 0.001$ (*) was considered statistically significant with respect to the accumulation of control nanoliposomes. (b) Tumor volume as a function of treatment with GEM-loaded TSH-nanoliposomes and control nanoliposomes ($n = 5$/group). Statistical analysis: *, $p < 0.01$ vs. control; **, $p < 0.001$ vs. control; ##, $p < 0.001$ vs. GEM-loaded nanoliposomes. (c) Weight of tumors 15 days after treatment initiation ($n = 5$/group). Statistical analysis: *, $p < 0.001$ vs. control; ##, $p < 0.001$ GEM-loaded nanoliposomes. (d) Photographs of dissected tumors 15 days after treatment initiation.

be used to deliver a variety of therapeutic agents. In particular, both hydrophilic and hydrophobic therapeutics can be loaded inside liposomes [33–36]. For instance, TSH-nanoliposomes could also be used for the delivery of antithyroid drugs to benign lesions, such as thyroid hyper-functioning adenomas [37].

4. Conclusions

We have developed a nanodelivery system consisting of nanoliposomes conjugated to the TSH. This delivery system is designed to target cells expressing the TSHr, which is frequently found in normal thyroid tissue and in a large number of thyroid carcinomas. Indeed, TSH-nanoliposomes displayed increased cellular uptake in comparison to control nanoliposomes in cells with TSHr. In addition, targeted nanoliposomes had higher levels of accumulation in normal thyroid tissue and in subcutaneous thyroid tumors. Furthermore when TSH-nanoliposomes were loaded with gemcitabine the *in vitro* and *in vivo* anticancer efficacy was markedly improved. Herein, we have demonstrated a valid delivery platform for obtaining enhanced deposition of drugs in thyroid tissue following systemic injection.

Conflict of interest disclosure

The authors declare no competing financial interests.

Acknowledgments

This paper was financially supported by the PON a3_00359 (IRC-FSH) Centro Interregionale per la Sicurezza degli Alimenti e la Salute, PRIN 2010-2011-prot. 2010H834LS_006 and Fondazione Umberto Di Mario ONLUS.

Appendix A. Supplementary data

Supplementary data related to this article can be found online at http://dx.doi.org/10.1016/j.biomaterials.2014.04.088.

References

[1] Fanciullino R, Ciccolini J. Nanoliposome-encapsulated anticancer drugs: still waiting for the magic bullet? Curr Med Chem 2009;16:4361–71.
[2] Ferrari M. Cancer nanotechnology: opportunities and challenges. Nat Rev Cancer 2005;5:161–71.

[3] Tao L, Hu W, Liu Y, Huang G, Sumer BD, Gao J. Shape-specific polymeric nanomedicine: emerging opportunities and challenges. Exp Biol Med (Maywood) 2011;236:20–9.
[4] Paolino D, Cosco D, Licciardi M, Giammona G, Fresta M, Cavallaro G. Polyaspartylhydrazide copolymer-based supramolecular vesicular aggregates as delivery devices for anticancer drugs. Biomacromolecules 2008;9:1117–30.
[5] Celia C, Cosco D, Paolino D, Fresta M. Gemcitabine-loaded innovative nanocarriers vs GEMZAR: biodistribution, pharmacokinetic features and in vivo antitumor activity. Expert Opin Drug Deliv 2011;8:1609–29.
[6] Cosco D, Bulotta A, Ventura M, Celia C, Calimeri T, Perri G, et al. In vivo activity of gemcitabine-loaded PEGylated small unilamellar nanoliposomes against pancreatic cancer. Cancer Chemother Pharmacol 2009;64:1009–20.
[7] Celia C, Trapasso E, Locatelli M, Navarra M, Ventura CA, Wolfram J, et al. Anticancer activity of liposomal bergamot essential oil (BEO) on human neuroblastoma cells. Colloids Surf B Biointerfaces 2013;112:548–53.
[8] Celia C, Ferrati S, Bansal S, van de Ven AL, Ruozi B, Zabre E, et al. Sustained zero-order release of intact ultra-stable drug-loaded nanoliposomes from an implantable nanochannel delivery system. Adv Healthc Mater 2014;3:230–8.
[9] Pasut G, Veronese FM. State of the art in PEGylation: the great versatility achieved after forty years of research. J Control Release 2012;161:461–72.
[10] Pasut G, Veronese FM. PEGylation for improving the effectiveness of therapeutic biomolecules. Drugs Today (Barc) 2009;45:687–95.
[11] Wolfram J, Suri K, Yang Y, Shen J, Celia C, Fresta M, et al. Shrinkage of pegylated and non-pegylated nanoliposomes in serum. Colloids Surf B Biointerfaces 2014;114:294–300.
[12] Gentile E, Cilurzo F, Di Marzio L, Carafa M, Ventura CA, Wolfram J, et al. Liposomal chemotherapeutics. Future Oncol 2013;9:1849–59.
[13] Shmeeda H, Tzemach D, Mak L, Gabizon A. Her2-targeted pegylated liposomal doxorubicin: retention of target-specific binding and cytotoxicity after in vivo passage. J Control Release 2009;136:155–60.
[14] Koren E, Apte A, Jani A, Torchilin VP. Multifunctional PEGylated 2C5-immunonanoliposomes containing pH-sensitive bonds and TAT peptide for enhanced tumor cell internalization and cytotoxicity. J Control Release 2012;160:264–73.
[15] Paolino D, Licciardi M, Celia C, Giammona G, Fresta M, Cavallaro G. Folate-targeted supramolecular vesicular aggregates as a new frontier for effective anticancer treatment in in vivo model. Eur J Pharm Biopharm 2012;82:94–102.
[16] Licciardi M, Paolino D, Celia C, Giammona G, Cavallaro G, Fresta M. Folate-targeted supramolecular vesicular aggregates based on polyaspartylhydrazide copolymers for the selective delivery of antitumoral drugs. Biomaterials 2010;31:7340–54.
[17] El-Kaissi S, Wall JR. Targeting the thyrotropin receptor in thyroid disease. Expert Opin Ther Targets 2012;16:719–27.
[18] Lazar V, Bidart JM, Caillou B, Mahé C, Lacroix L, Filetti S, et al. Expression of the Na+/I− symporter gene in human thyroid tumors: a comparison study with other thyroid-specific genes. J Clin Endocrinol Metab 1999;84:3228–34.
[19] Durante C, Puxeddu E, Ferretti E, Morisi R, Moretti S, Bruno R, et al. BRAF mutations in papillary thyroid carcinomas inhibit genes involved in iodine metabolism. J Clin Endocrinol Metab 2007;92:2840–3.
[20] Schlumberger M, Lacroix L, Russo D, Filetti S, Bidart JM. Defects in iodide metabolism in thyroid cancer and implications for the follow-up and treatment of patients. Nat Clin Pract Endocrinol Metab 2007;3:260–9.
[21] Brabant G, Maenhaut C, Köhrle J, Scheumann G, Dralle H, Hoang-Vu C, et al. Human thyrotropin receptor gene-expression in thyroid tumors and correlation to markers of thyroid differentiation and dedifferentiation. Mol Cell Endocrinol 1991;82(1):R7–12.
[22] Tanaka K, Otsuki T, Sonoo H, Yamamoto Y, Udagawa K, Kunisue H, et al. Semiquantitative comparison of the differentiation markers and sodium iodide symporter messenger ribonucleic acids in papillary thyroid carcinomas using RT-PCR. Eur J Endocrinol 2000;142:340–6.
[23] Gérard AC, Daumerie C, Mestdagh C, Gohy S, De Burbure C, Costagliola S, et al. Correlation between the loss of thyroglobulin iodination and the expression of thyroid-specific proteins involved in iodine metabolism in thyroid carcinomas. J Clin Endocrinol Metab 2003;88:4977–83.
[24] Gaspari M, Abbonante V, Cuda G. Gel-free sample preparation for the nanoscale LC-MS/MS analysis and identification of low-nanogram protein samples. J Sep Sci 2007;30:2210–6.
[25] Paolino D, Lucania G, Mardente D, Alhaique F, Fresta M. Ethosomes for skin delivery of ammonium glycyrrhizinate: in vitro percutaneous permeation through human skin and in vivo anti-inflammatory activity on human volunteers. J Control Release 2005;106:99–110.
[26] Wadsworth HL, Russo D, Nagayama Y, Chazenbalk GD, Rapoport B. Studies on the role of amino acids 38-45 in the expression of a functional thyrotropin receptor. Mol Endocrinol 1992;6:394–8.
[27] Kim WG, Zhao L, Kim DW, Willingham MC, Cheng SY. Inhibition of tumorigenesis by the thyroid hormone receptor β in xenograft models. Thyroid 2014;24:260–9.
[28] Paolino D, Cosco D, Molinaro R, Celia C, Fresta M. Supramolecular devices to improve the treatment of brain diseases. Drug Discov Today 2011;16:311–24.
[29] Celia C, Cosco D, Paolino D, Fresta M. Nanoparticulate devices for brain drug delivery. Med Res Rev 2011;31:716–56.
[30] Paolino D, Cosco D, Racanicchi L, Trapasso E, Celia C, Iannone M, et al. Gemcitabine-loaded PEGylated unilamellar nanoliposomes vs GEMZAR: biodistribution, pharmacokinetic features and in vivo antitumor activity. J Control Release 2010;144:144–50.
[31] Celano M, Calvagno MG, Bulotta S, Paolino D, Arturi F, Rotiroti D, et al. Cytotoxic effects of gemcitabine-loaded nanoliposomes in human anaplastic thyroid carcinoma cells. BMC Cancer 2004;4:63.
[32] Celia C, Calvagno MG, Paolino D, Bulotta S, Ventura CA, Russo D, et al. Improved in vitro anti-tumoral activity, intracellular uptake and apoptotic induction of gemcitabine-loaded pegylated unilamellar nanoliposomes. J Nanosci Nanotechnol 2008;8:2102–13.
[33] Schwendener RA. Nanoliposomes in biology and medicine. Adv Exp Med Biol 2007;620:117–28.
[34] Saad M, Garbuzenko OB, Minko T. Co-delivery of siRNA and an anticancer drug for treatment of multidrug-resistant cancer. Nanomedicine (Lond) 2008;3:761–76.
[35] Cosco D, Paolino D, Cilurzo F, Casale F, Fresta M. Gemcitabine and tamoxifen-loaded nanoliposomes as multidrug carriers for the treatment of breast cancer diseases. Int J Pharm 2012;422:229–37.
[36] Torchilin VP. Recent advances with nanoliposomes as pharmaceutical carriers. Nat Rev Drug Discov 2005;4:145–60.
[37] Azizi F. The safety and efficacy of antithyroid drugs. Expert Opin Drug Saf 2006;5:107–16.